HHS Public Access

Author manuscript

J Invest Dermatol. Author manuscript; available in PMC 2015 August 01.

Published in final edited form as:

J Invest Dermatol. 2015 February ; 135(2): 462–470. doi:10.1038/jid.2014.378.

Fatty Acid Transport Protein 1 can compensate for Fatty Acid Transport Protein 4 in the developing mouse epidermis

Meei-Hua Lin[1] and **Jeffrey H. Miner**[1,2]

[1]Renal Division, Washington University, School of Medicine, St. Louis, Missouri, USA

[1,2]Department of Cell Biology and Physiology, Washington University, School of Medicine, St. Louis, Missouri, USA

SUMMARY

Fatty acid transport protein (FATP) 4 is one of a family of six FATPs that facilitate long- and very long-chain fatty acid uptake. Mice lacking FATP4 are born with tight, thick skin and a defective barrier; they die neonatally due to dehydration and restricted movements. Mutations in *SLC27A4*, the gene encoding FATP4, cause ichthyosis prematurity syndrome (IPS), characterized by premature birth, respiratory distress, and edematous skin with severe ichthyotic scaling. Symptoms of surviving patients become mild, though atopic manifestations are common. We previously showed that suprabasal keratinocyte expression of a Fatp4 transgene in *Fatp4* mutant skin rescues the lethality and ameliorates the skin phenotype. Here we tested the hypothesis that FATP1, the closest FATP4 homolog, can compensate for the lack of FATP4 in our mouse model of IPS, as it might do postnatally in IPS patients. Transgenic expression of FATP1 in suprabasal keratinocytes rescued the phenotype of *Fatp4* mutants, and FATP1 sorted to the same intracellular organelles as endogenous FATP4. Thus, FATP1 and FATP4 likely have overlapping substrate specificities, enzymatic activities, and biological functions. These results suggest that increasing expression of FATP1 in suprabasal keratinocytes could normalize the skin of IPS patients and perhaps prevent the atopic manifestations.

Keywords

Fatty acids; fatty acid transport; skin barrier; epidermis

INTRODUCTION

Mammalian skin provides the first line of defense against mechanical, chemical, and biological assaults and functions as a barrier to inhibit water loss. The cutaneous permeability barrier is mediated by the most superficial, cornified epidermal layer that forms

Correspondence: Jeffrey H. Miner, Renal Division 8126, 660 S. Euclid Ave., St. Louis, MO, 63110, USA. Tel: 314-362-8235; Fax: 314-362-8237; minerj@wustl.edu.

CONFLICT OF INTEREST

None to disclose

from a series of differentiation and stratification processes. At the beginning of epidermal differentiation, proliferative basal keratinocytes migrate suprabasally and switch from a keratins 5/14-containing network to a keratins 1/10-containing network, forming the spinous layer (Candi *et al.*, 2005). The granular layer above has profilaggrin-containing keratohyalin granules that facilitate the assembly of keratin bundles. Granulocytes form a cornified envelope beneath the cell membrane via the cross-linking of involucrin (IVL), loricrin, and other proteins (Candi et al., 2005). The cornified layer consists of dead, flattened, interdigitating keratinocytes embedded in a lipid-rich matrix that results from secretion and processing of lipids from lamellar bodies in granulocytes (Breiden and Sandhoff, 2013).

Fatty acids in either a complex lipid or a free form are crucial to the epidermal permeability barrier. Fatty acids serve as building blocks for the complex lipids necessary to form the permeability barrier, as signals for keratinocytes to regulate epidermal homeostasis, and as acidifiers of the cornified layer to promote its structural integrity and barrier function (Lin and Khnykin, 2013). Fatty acids can be synthesized *de novo* by keratinocytes or taken up from the diet or from extracutaneous sites. Several proteins facilitate the uptake of long-chain fatty acids in mammalian cells, including fatty acid translocase (Coburn *et al.*, 2001; Furuhashi and Hotamisligil, 2008), fatty acid binding protein (Furuhashi and Hotamisligil, 2008), and members of the fatty acid transport protein/very long-chain acyl-CoA synthetase (FATP/ACSVL) family (Anderson and Stahl, 2013; Gimeno, 2007). However, the exact molecular mechanism of transport across the plasma membrane remains unclear. Clinical findings and recent studies in animal models suggest crucial roles for these candidate transporters in the skin (Lin and Khnykin, 2013).

The FATP family consists of six membrane proteins that can all facilitate uptake of fatty acids of 16 to 24 carbons (Coe *et al.*, 1999; Hall *et al.*, 2005; Jia *et al.*, 2007; Mihalik *et al.*, 2002). FATPs display acyl-CoA synthetase (ACS) activity and are proposed to facilitate uptake of fatty acids by a mechanism called vectorial acylation, whereby free fatty acids are esterified into an acyl-CoA form after import, thus diminishing the intracellular pool of free fatty acids and creating a gradient across the membrane that drives their further influx (Black and DiRusso, 2003). It is not known whether FATPs function as inherent transporters or whether a different protein is required to facilitate fatty acid import. The distribution of FATPs in the skin varies substantially: FATP1, FATP3, FATP4, and FATP6 are detected in the epidermis and hair follicles of adult mice; FATP1 and FATP4 are robustly expressed in subcutaneous fat; and FATP4 is the only FATP detected in sebaceous glands (Schmuth *et al.*, 2005).

We previously identified an autosomal recessive mouse phenotype called *wrinkle free* caused by a retrotransposon insertion into *Slc27a4*, the gene encoding FATP4 (Moulson *et al.*, 2003). Mice lacking FATP4 (herein referred to as $Fatp4^{-/-}$ mice) are born with tight, thick, “wrinkle free” skin and a defective skin barrier, whereas $Fatp4^{+/-}$ mice are phenotypically normal. $Fatp4^{-/-}$ mice die neonatally due to dehydration and restricted movements. Similar phenotypes occur in two independently derived *Fatp4* mutants (Herrmann *et al.*, 2003; Tao *et al.*, 2012). Suprabasal keratinocyte expression of a Fatp4 transgene in *Fatp4* mutant skin rescues the neonatal lethality and ameliorates the skin

phenotype, underscoring the crucial, skin-intrinsic roles of FATP4 in skin development and function (Moulson *et al.*, 2007).

Mutations affecting human FATP4 occur in patients with ichthyosis prematurity syndrome (IPS), characterized by premature birth, respiratory distress, peripheral blood eosinophilia, and edematous skin with severe caseous scaling (Bygum *et al.*, 2008; Klar *et al.*, 2009; Sobol *et al.*, 2011). Symptoms of surviving patients become mild during childhood and manifest mainly as dry and pruritic skin, though respiratory and/or food allergies are common (Khnykin *et al.*, 2012). This suggests that FATP4 is critical for the development of skin during the fetal and neonatal periods, but other FATPs may compensate for the lack of FATP4 at later stages.

Here we tested the hypothesis that FATP1, the FATP with the highest homology to FATP4, can functionally compensate for the lack of FATP4. Our results demonstrate that transgenic FATP1 expression in suprabasal keratinocytes rescues the neonatal lethality and ameliorates the skin phenotype in *Fatp4* mutants, similar to transgenic FATP4 expression.

RESULTS

Expression of *Fatp4* and *Fatp1* in fetal skin

By in situ hybridization, *Fatp4* was normally expressed in fetal epidermis in suprabasal keratinocytes (upper left panel in Figure 1a) and in hair follicle and sebaceous gland progenitors (Lin *et al.*, 2013). In contrast, $Fatp4^{-/-}$ mice showed nuclear localization of Fatp4 RNA in some epidermal keratinocytes, perhaps due to mislocalization of mutant transcripts caused by inclusion of the retrotransposon (upper middle panel in Figure 1a) (Lin et al., 2013). FATP1 is the FATP with the highest homology to FATP4 (Hirsch *et al.*, 1998). Fatp1 RNA was detected in subsets of basal keratinocytes, in hair follicle progenitors (lower left panel in Figure 1a), and in subcutaneous adipocytes (data not shown) during fetal development. Its epidermal expression did not appear to be affected by the lack of FATP4 (lower middle panel in Figure 1a). Thus, *Fatp4* and *Fatp1* are expressed in nearly complementary compartments in fetal mouse skin.

Restoration of the skin barrier in $Fatp4^{-/-}$;Tg(IVL-Fatp1) mice

We showed previously that suprabasal keratinocyte expression of a Fatp4 transgene in *Fatp4* mutant skin rescues the neonatal lethality and ameliorates the skin phenotype, underscoring the crucial, skin-intrinsic roles of FATP4 in the development and function of skin (Moulson et al., 2007). To test whether FATP1 can functionally compensate for the lack of FATP4 in our mouse model of IPS, we generated three independent lines of transgenic mice expressing a hemagglutinin (HA)-tagged FATP1 under the control of the human *IVL* promoter. After crossing to $Fatp4^{+/-}$ mice for two generations, $Fatp4^{-/-}$;Tg(IVL-Fatp1) mice were obtained. $Fatp4^{-/-}$;Tg(IVL-Fatp1) mice derived from two of the transgenic lines were viable and fertile and showed robust Fatp1 transgene expression in suprabasal keratinocytes (lower right panel in Figure 1a). While Fatp1 RNA in early hair follicle progenitors was decreased in $Fatp4^{-/-}$;Tg(IVL-Fatp1) skin (lower right panel in Figure 1a), its expression in more differentiated follicles was not changed (not shown). Like

Fatp4$^{-/-}$;Tg(IVL-Fatp4) mice (Moulson et al., 2007), *Fatp4*$^{-/-}$;Tg(IVL-Fatp1) mice also displayed disheveled coat hair as early as around weaning age, which progressed into thinning hair and/or patches of alopecia at older ages (data not shown). *Fatp4*$^{-/-}$ mice rescued by either of the two IVL-Fatp1 lines showed similar results; data obtained from one line are shown here. *Fatp4*$^{-/-}$;Tg(IVL-Fatp1) mice from the third line died postnatally due to transgene expression in only a subset of granular cells (data not shown).

Fatp4$^{-/-}$ mice exhibit an abnormal permeability barrier from E16.5 onwards and show an incomplete barrier at birth; these barrier defects are remedied by expression of a Fapt4 transgene in suprabasal keratinocytes (Lin *et al.*, 2010; Moulson et al., 2007). As assayed by the inward permeability of X-Gal, forced FATP1 expression in the epidermis was also able to normalize the defective barrier of *Fatp4*$^{-/-}$ fetuses (Figure 1b). Moreover, *Fatp4*$^{-/-}$ newborns showed a significantly higher outward transepidermal water loss (TEWL) than *Fatp4*$^{+/-}$ controls (5.3±1.6 g/m^{2}h, n=9 vs. 1.1±0.9 g/m^{2}h, n=4; ***P<0.001) (Figure 1c). However, *Fatp4*$^{-/-}$;Tg(IVL-Fatp1) newborns displayed a TEWL that was indistinguishable from that of *Fatp4*$^{+/-}$ controls (1.2±0.9 g/m^{2}h, n=8; P>0.05) (Figure 1c). The statistically significant reduction in TEWL by Fatp1 transgene expression was also observed in *Fatp4*$^{-/-}$;Tg(IVL-Fatp4) newborns (Figure 1d). The permeability barrier in *Fatp4*$^{+/-}$;Tg(IVL-Fatp1) and *Fatp4*$^{+/-}$;Tg(IVL-Fatp4) mice was indistinguishable from that of *Fatp4*$^{+/-}$ mice (Figure 1b–d). These results demonstrate that forced ectopic expression of FATP1 in *Fatp4*$^{-/-}$ suprabasal keratinocytes rescues the neonatal lethality and restores the permeability barrier.

Amelioration of skin phenotypes in *Fatp4*$^{-/-}$;Tg(IVL-Fatp1) mice

Fatp4$^{-/-}$ fetuses display epidermal hyperplasia that results from an increased number of proliferating suprabasal cells (Lin et al., 2010). The hyperplasia is associated with epidermal activation of keratin 6 expression, epidermal growth factor receptor (EGFR) signaling, and phosphorylation and nuclear translocation of STAT3, a downstream effector of EGFR signaling. Pharmacological inhibition of EGFR and STAT3 activation reduce skin thickening and partially suppress the barrier abnormalities (Lin et al., 2010). Consistent with the RNA expression pattern of the Fatp1 transgene, HA-tagged FATP1 was detected specifically in suprabasal keratinocytes (second row in Figure 2). The transgenic FATP1 prevented the epidermal hyperplasia observed in *Fatp4*$^{-/-}$ mice (top row in Figure 2). In addition, the ectopic activation of keratin 6 and STAT3 in *Fatp4*$^{-/-}$ epidermis was diminished by Fatp1 transgene expression (bottom two rows in Figure 2). This amelioration of *Fatp4*$^{-/-}$ skin phenotypes is reminiscent of the effects of suprabasal Fatp4 transgene expression (Moulson et al., 2007).

Amelioration of lipid abnormalities in *Fatp4*$^{-/-}$;Tg(IVL-Fatp1) epidermis

FATP4 is normally localized to the granular layer of the epidermis, where barrier lipid precursors are synthesized. During epidermal differentiation, the lipid-enriched contents of lamellar bodies in the uppermost cells of the granular layer are secreted into the extracellular space and processed into ceramides, cholesterol, and fatty acids, the three major lipids required for permeability barrier function of the cornified layer (Holleran *et al.*, 2006). Epidermal lipid analyses of *Fatp4* mutant newborns revealed a significantly decreased

proportion of ceramides with fatty acid moieties containing 26 or more carbon atoms and a significantly increased proportion of those containing 24 or fewer carbon atoms (Herrmann et al., 2003; Moulson et al., 2007). These ceramide abnormalities suggest an inability of *Fatp4* mutant keratinocytes to activate very long-chain fatty acids to an acyl-CoA form, which could lead to subsequent accumulation of free fatty acids inside cells.

To investigate this hypothesis, we performed lipid analyses by thin layer chromatography (TLC) using total free, extractable lipids isolated from newborn epidermis. Compared to controls, *Fatp4*$^{-/-}$ epidermis showed a significantly increased amount of free fatty acids (Figure 3). Quantification of free fatty acids in separate studies revealed 4.44 ± 0.82 μg/mg dry tissue in controls (n=4) vs. 8.80 ± 1.75 μg/mg in mutants (n=4), $P<0.01$ (Table S1a); and 3.96 ± 1.06 μg/mg dry tissue in controls (n=6) vs. 6.54 ± 0.82 μg/mg in mutants (n=6), $P<0.001$ (Table S1b). Furthermore, these increases were ameliorated in both *Fatp4*$^{-/-}$;Tg(IVL-Fatp1) mice (Figure 3a and Table S1a) and *Fatp4*$^{-/-}$;Tg(IVL-Fatp4) mice (Figure 3b and Table S1b). In contrast, the levels of cholesteryl ester, triacyglycerol, and free cholesterol in the newborn epidermis were not significantly affected by FATP4 deficiency (Figure 3 and Table S1).

Subcellular localization of endogenous FATP4 and transgenic FATP1 in the epidermis

The subcellular localization of FATP1 and FATP4 in mammalian cells has been reported to be plasma membrane and/or intracellular organelles (Kazantzis and Stahl, 2012 and references therein). For example, studies of stably transfected FATP4-overexpressing cells suggest that FATP4 is an endoplasmic reticulum (ER)-localized ACS that is able to drive import of fatty acids via its enzymatic activity (Milger *et al.*, 2006; Zhan *et al.*, 2012). Our previous study of cultured fibroblasts shows that endogenous FATP4 is localized to mitochondria and to a lesser extent to ER and peroxisomes (Jia et al., 2007). To examine whether endogenous FATP4 is also localized to multiple organelles in the epidermis, granular keratinocytes, which show the most intense FATP4 immunostaining (Lin et al., 2013), were isolated from newborn and young pup skin and analyzed.

By hematoxylin staining, granular keratinocytes isolated from control mice were filled with keratohyalin granules (lower left panel in Figure 4). Compared to controls, granular keratinocytes from *Fatp4*$^{-/-}$ newborns were smaller, and the granules were less distinct (middle column in Figure 4). In contrast, these abnormalities were remedied in *Fatp4*$^{-/-}$;Tg(IVL-Fatp4) cells and *Fatp4*$^{-/-}$;Tg(IVL-Fatp1) cells (right column in Figure 4). By double immunofluorescence staining, endogenous FATP4 in control cells was detected in a mesh-like pattern that colocalized mainly with the ER luminal protein calreticulin (Figure 5d–f′) and partially with the mitochondrial membrane protein ATP synthase (Figure 5a–c′; arrowheads in c′). The FATP4 signals were also observed at the nuclear surface, which is very likely the ER membrane that is contiguous with the nuclear membrane. Using interleukin 1 receptor 1 as a marker, we could not detect FATP4 at the plasma membrane (Figure 5g–i′). The mesh-like pattern of FATP4 staining was similar to the inter-granular staining of calreticulin (Figure 5j–l′). FATP4 was not detected in *Fatp4*$^{-/-}$ cells (Figure 5p–r′ and data not shown).

As demonstrated above, transgenic expression of FATP1 in suprabasal keratinocytes rescued the *Fatp4*−/− neonatal lethality and normalized most of the skin abnormalities. To examine whether the rescuing effects of exogenous FATP1 correlated with its trafficking to the same subcellular compartments as endogenous FATP4, granular keratinocytes from *Fatp4*$^{+/+}$;Tg(IVL-Fatp1) mice were subjected to double immunofluorescence staining with HA-tag and FATP4 antibodies. As shown in Figure 5s–u′, HA-tagged transgenic FATP1 colocalized nearly completely with endogenous FATP4. This implies localization of transgenic FATP1 to ER and mitochondria but not to the plasma membrane, as observed for FATP4. This observation was confirmed by double immunofluorescence staining in *Fatp4*$^{-/-}$;Tg(IVL-Fatp1) cells with HA-tag antibody and various organellar marker antibodies (Figure S1). These results suggest that the rescuing effects of HA-FATP1 require its sorting to the same subcellular compartments as FATP4.

DISCUSSION

Among the six mouse FATP family members, FATP1 is most closely related to FATP4 (Herrmann *et al.*, 2001). These two FATPs are expressed in nearly complementary compartments in the skin during fetal development: FATP4 in suprabasal keratinocytes, sebaceous gland progenitors, and hair follicle progenitors (Lin et al., 2013), and FATP1 in cell clusters within the basal layer of the epidermis, in adipocytes of subcutaneous fat, and in hair follicle progenitors (Figure 1). Unlike *Fatp4*$^{-/-}$ mice, knockout of *Fatp1* does not lead to skin phenotypes, despite its cutaneous expression pattern (Kim *et al.*, 2004). In addition, although FATP4 expression predominates in fetal mouse epidermis, FATP1 expression predominates in adult epidermis (Schmuth et al., 2005). The spatial and temporal differences in expression of these two FATPs in the skin suggest regulation to meet the metabolic requirements of various compartments and developmental stages.

Our results demonstrate that transgenic expression of FATP1 in suprabasal keratinocytes of *Fatp4*$^{-/-}$ mice, like that of FATP4, rescues the neonatal lethality and normalizes the permeability barrier, epidermal hyperplasia, the level of free fatty acids, epidermal activation of keratin 6 and STAT3, and defective keratohyalin granules. The subcellular localization of FATP1 and FATP4 in mammalian cells has been reported to be plasma membrane and/or intracellular organelles (Kazantzis and Stahl, 2012 and references therein). However, our results show that endogenous FATP4 in epidermal keratinocytes is localized to the ER and mitochondria, but not to the plasma membrane. This suggests that in epidermal keratinocytes FATP4 does not function as a transmembrane transporter *per se*, but rather facilitates fatty acid import indirectly by activating fatty acids to an acyl-CoA form. Studies using FATP4-overexpressing cells suggest that FATP4 is an ER-localized ACS that displays a type III signal-anchor transmembrane domain topology, with the short N-terminal sequence of FATP4 oriented toward the ER lumen and the enzymatic part facing the cytosolic side (Milger et al., 2006; Zhan et al., 2012). It remains unknown how the information in FATP4 regulates its targeting in epidermal keratinocytes to the ER and to the mitochondria, but our results show that exogenous FATP1 was sorted to these same granular keratinocyte subcellular compartments.

Our preliminary mass spectrometry data show that the elevated free fatty acid pool in *Fatp4*$^{-/-}$ epidermis (Figure 3) was composed of VLCFA, especially C22:0, C24:0, C24:1, and C26:1. The increases in these VLCFA were normalized by both Fatp1 and Fatp4 transgenes (unpublished data). Taken together, that FATP1 could functionally compensate for the FATP4 deficiency in *Fatp4*$^{-/-}$ skin indicates that FATP1 and FATP4 likely share similar substrate specificities and enzymatic activities. The presence of both genes in the mammalian genome could relate to their partially non-overlapping expression patterns rather than to any significant functional differences.

As in adult mouse epidermis, FATP1, -3, -4, and -6 are also expressed in human epidermis. Upon barrier disruption in adult mice, the epidermal expression of FATP6 and fatty acid translocase, another candidate transporter that facilitates the uptake of fatty acids in the epidermis, is increased. This upregulation suggests potential roles for FATPs in restoring the steady state of barrier lipids (Schmuth et al., 2005). It would be important to investigate whether in IPS patients other FATPs or other candidate transporters are ectopically expressed in the same epidermal compartments as endogenous FATP4 after birth to compensate for the skin abnormalities. Given the functional similarities between FATP1 and FATP4 revealed by our mouse studies, increasing expression of *FATP1/SLC27A1* in suprabasal keratinocytes could be pursued as a therapy to normalize the skin phenotype of IPS patients and perhaps prevent the development of atopic manifestations. Our results in mice also suggest that the amelioration of symptoms in IPS patients postnatally might be attributable to postnatal ectopic expression of *FATP1* in the cell layer where endogenous *FATP4* is normally expressed. In *Fatp4* mutant mice, the epidermal expression of Fatp1 RNA during fetal development (Figure 1) or at birth (data not shown) did not appear to be increased by the lack of FATP4, perhaps explaining their severe skin phenotype.

MATERIALS AND METHODS

Mice

Fatp4 mutant and *IVL* promoter-driven Fatp4 transgenic mice have been previously described (Moulson et al., 2007; Moulson et al., 2003). The human *IVL* promoter-driven Fatp1 transgene was generated by PCR amplification of a cDNA encoding FATP1 with an amino-terminal hemagglutinin (HA)-tag (Chiu *et al.*, 2005) using Klentaq LA DNA polymerase (in-house facility of Washington University) and primers that added NotI sites to the HA-tag and to the 3′ end of the cDNA. The PCR product was purified by the Wizard SV Gel and PCR CleanUp System (Promega, Madison, WI), cut with NotI, and ligated into the NotI sites of a clone containing the human *IVL* promoter and the SV40 polyadenylation signal sequence (Carroll *et al.*, 1993). The transgene was liberated from the vector by digestion with *Sal*I and purified by the QIAEX II Gel Extraction Kit (Qiagen, Germantown, MD). Transgenic mice were generated by microinjection of the transgene into the pronuclei of one-cell stage B6CBAF2/J mouse embryos. Potential founders were screened for incorporation of the transgene by PCR using primers from two different exons of *Fatp1* and examined for expression of the transgene by immunohistochemistry with an HA tag antibody (see below). Embryos were dissected from pregnant females, with the morning

when the copulation plug was observed considered embryonic day (E) 0.5. All experiments were approved by the Washington University Animal Studies Committee.

Skin barrier assays

Inward permeability assay by X-Gal and outward TEWL assay with a Vapometer were performed as described (Lin et al., 2010).

Immunohistochemistry

Immunohistochemical analyses on paraffin sections were performed as described (Lin et al., 2010). The antigen retrieval method and dilutions of primary antibodies used were as follows: EDTA and 1:50 for phospho-STAT3 (Tyr705); Trilogy and 1:50 for HA tag (both antibodies from Cell Signaling Technology, Beverly, MA); and 1:1,000 for keratin 6 (Covance, Princeton, NJ). Sections were counterstained with hematoxylin and mounted.

In situ hybridization

Preparation of paraffin sections and in situ hybridization using digoxigenin-UTP labeled Fatp4 and Fatp1 riboprobes were performed as described (Moulson et al., 2007), with the hybridization temperature at 60°C and 55°C, respectively.

Extraction of epidermal lipids

HPLC grade solvents were purchased from Sigma Chemical Co. (St. Louis, MO). Free, extractable lipids were isolated from the epidermis of newborn mice. To isolate the epidermis, the body trunk skin was incubated in 10 mM EDTA in PBS at 37°C for 1.5 h with the dermal side down. The epidermis was peeled as a whole sheet, lyophilized, weighed, and stored at −80°C. Lipids were extracted from lyophilized epidermis of each newborn with 3.8 ml of chloroform/methanol/water (1/2/0.8) at room temperature for 2 h followed by phase separation by adding 1 ml each of chloroform and water. After centrifugation, the lipid-enriched lower phase was reextracted with 1 ml of chloroform, 1 ml of methanol, and 0.9 ml of water and recentrifuged. The lower phase was then dried with a nitrogen evaporator (Organomation Associates, Inc., Berlin, MA), resuspended in 200 μl chloroform/methanol (2/1), and stored under nitrogen at −20°C.

Lipid analysis by TLC

Silica gel 60 plates (Sigma; Merck, Germany) were baked at 120°C for 30 min in an oven prior to use. To separate neutral lipids, lipid extracts were applied to plates and resolved in a solvent mixture of hexane/diethyl ether/acetic acid (70:30:1) in a pre-equilibrated tank until the solvent front reached the top of the plate (20 cm). Standard lipids used include the non-polar lipid mix B, palmitic acid (16:0) (both from Matreya LLC, Pleasant Gap, PA), heptacosanoic acid (27:0), and a mono-, di-, triglyceride mix (both from Sigma). Resolved plates were dried, and the lipid spots were visualized by spraying with 3% copper acetate in 8% phosphoric acid followed by charring at 180°C for 15 min in an oven (Macala *et al.*, 1983). For quantification of lipid species, lipid spots on charred TLC plates were scanned and quantified in ImageJ (http://rsbweb.nih.gov/ij/) with co-chromatographed standards in

the range of 0.5 to 4 μg for each band. Cholesteryl oleate, triolein, and oleic acid were used as the standards for cholesteryl ester, triacylglycerol, and free fatty acids, respectively.

Isolation of keratinocyte fractions

The epidermis was collected from newborn mice and young pups up to 5.5 days of age as described above. For newborns, the basal and spinous keratinocytes-enriched fraction was obtained by incubating the epidermis in 0.05% trypsin-EDTA (Gibco, Grand Island, NY) at 37°C for 20 min in a small dish with the skin surface up followed by manually shaking the digested epidermis in cold PBS vigorously 20 times and filtering through a 70-μm nylon cell strainer (BD Biosciences, San Jose, NJ) into a tube containing cold soy bean trypsin inhibitor (Gibco) at 0.5 mg/ml in PBS. The granular keratinocytes-enriched fraction was obtained by incubating the residual epidermal sheet in 0.25% trypsin-EDTA (Gibco) at 37°C for 20 min in a small dish with the skin surface up followed by manually shaking the digested sheet in cold trypsin inhibitor solution vigorously 20 times and filtering through a 100-μm nylon cell strainer (BD Biosciences). Both cell fractions were then centrifuged at 800 rpm for 5 min at 4°C, resuspended in cold PBS, and spun onto slides at 400 rpm for 3 min in a Shandon Cytospin (Thermo Scientific, Rockford, IL) to make a cell monolayer. Slides were air dried for 10 min and stored at −20°C for up to a week.

Immunofluorescence staining

The cell monolayers were fixed in 4% paraformaldehyde in PBS for 5 min, permeabilized with cold methanol at −20°C for 5 min, and blocked in 1% bovine serum albumin and 10% normal goat serum or normal donkey serum in PBS for 30 min. Cells were then incubated at 4°C overnight with primary antibodies diluted in 1% bovine serum albumin in PBS, incubated for 30 min in dark with fluorophore-labeled secondary antibodies diluted in 1% bovine serum albumin in PBS, counterstained with Hoechst 33258, and mounted in 90% glycerol containing 0.1X PBS and 1 mg/ml *p*-phenylenediamine. Immunostaining with filaggrin antibody was performed on freshly prepared cell monolayers by fixation in 4% paraformaldehyde in PBS for 20 min and permeabilization in 0.5% Triton X-100 in PBS for 5 min. Dilutions of primary antibodies used were as follows: 1:100 for FATP4 (Newberry *et al.*, 2003), calreticulin/calregulin (Santa Cruz Biotechnology, Santa Cruz, CA), ATP synthase, beta chain (Millipore, Temecula, CA), and interleukin 1 receptor 1 (R&D Systems, Minneapolis, MN); 1:4000 for filaggrin and 1:50 for mouse HA-tag (Covance, Princeton, NJ); 1:50 for rabbit HA-tag (Cell Signaling Technology, Beverly, MA). Fluorophore-conjugated secondary antibodies were used at a 1:400 dilution and included the following: goat Alexa 488 anti-rabbit; goat Cy3 anti-mouse (both from Invitrogen); donkey Alexa 488 anti-rabbit; donkey Cy3 anti-goat (both from Jackson Immunoresearch, West Grove, PA). Images were acquired with a Nikon C1 confocal system (Nikon Instruments, Melville, NY) and analyzed in Nikon Elements software (Nikon).

Statistical analysis

Two-tailed, unpaired Student's *t*-tests were used to determine statistical significance in the assays. Differences were considered significant when $P < 0.05$.

Supplementary Material

Refer to Web version on PubMed Central for supplementary material.

Acknowledgments

This work was supported by National Institutes of Health grant R01AR049269 (to JHM). We thank Darlene Stewart and Teresa Tolley for assistance with histology; Gloriosa Go for transgene preparation; Jennifer Richardson for mouse genotyping; and the Mouse Genetics Core for generating transgenic mice and for husbandry. Production of Fatp1 transgenic mice was supported by the Digestive Diseases Research Core Center (P30DK052574). The animals were housed in a facility supported by NCRR grant C06RR015502.

Abbreviations

ACS	acyl-CoA synthetase
ACSVL	very long chain acyl-CoA synthetase
E	embryonic day
ER	endoplasmic reticulum
FATP	fatty acid transport protein
HA	hemagglutinin
IPS	ichthyosis prematurity syndrome
IVL	involucrin
TEWL	transepidermal water loss
TLC	thin layer chromatography

References

Anderson CM, Stahl A. SLC27 fatty acid transport proteins. Mol Aspects Med. 2013; 34:516–528. [PubMed: 23506886]

Black PN, DiRusso CC. Transmembrane movement of exogenous long-chain fatty acids: proteins, enzymes, and vectorial esterification. Microbiol Mol Biol Rev. 2003; 67:454–472. table of contents. [PubMed: 12966144]

Breiden B, Sandhoff K. The role of sphingolipid metabolism in cutaneous permeabilitybarrier formation. Biochim Biophys Acta. 2013

Bygum A, Westermark P, Brandrup F. Ichthyosis prematurity syndrome: a well-defined congenital ichthyosis subtype. J Am Acad Dermatol. 2008; 59:S71–74. [PubMed: 19119129]

Candi E, Schmidt R, Melino G. The cornified envelope: a model of cell death in the skin. Nat Rev Mol Cell Biol. 2005; 6:328–340. [PubMed: 15803139]

Carroll JM, Albers KM, Garlick JA, et al. Tissue- and stratum-specific expression of the human involucrin promoter in transgenic mice. Proc Natl Acad Sci U S A. 1993; 90:10270–10274. [PubMed: 8234288]

Chiu HC, Kovacs A, Blanton RM, et al. Transgenic expression of fatty acid transport protein 1 in the heart causes lipotoxic cardiomyopathy. Circ Res. 2005; 96:225–233. [PubMed: 15618539]

Coburn CT, Hajri T, Ibrahimi A, et al. Role of CD36 in membrane transport and utilization of long-chain fatty acids by different tissues. J Mol Neurosci. 2001; 16:117–121. discussion 151–117. [PubMed: 11478366]

Coe NR, Smith AJ, Frohnert BI, et al. The fatty acid transport protein (FATP1) is a very long chain acyl-CoA synthetase. J Biol Chem. 1999; 274:36300–36304. [PubMed: 10593920]

Furuhashi M, Hotamisligil GS. Fatty acid-binding proteins: role in metabolic diseases and potential as drug targets. Nat Rev Drug Discov. 2008; 7:489–503. [PubMed: 18511927]

Gimeno RE. Fatty acid transport proteins. Curr Opin Lipidol. 2007; 18:271–276. [PubMed: 17495600]

Hall AM, Wiczer BM, Herrmann T, et al. Enzymatic properties of purified murine fatty acid transport protein 4 and analysis of acyl-CoA synthetase activities in tissues from FATP4 null mice. J Biol Chem. 2005; 280:11948–11954. [PubMed: 15653672]

Herrmann T, Buchkremer F, Gosch I, et al. Mouse fatty acid transport protein 4 (FATP4): characterization of the gene and functional assessment as a very long chain acyl-CoA synthetase. Gene. 2001; 270:31–40. [PubMed: 11404000]

Herrmann T, van der Hoeven F, Grone HJ, et al. Mice with targeted disruption of the fatty acid transport protein 4 (Fatp 4, Slc27a4) gene show features of lethal restrictive dermopathy. J Cell Biol. 2003; 161:1105–1115. [PubMed: 12821645]

Hirsch D, Stahl A, Lodish HF. A family of fatty acid transporters conserved from mycobacterium to man. Proc Natl Acad Sci U S A. 1998; 95:8625–8629. [PubMed: 9671728]

Holleran WM, Takagi Y, Uchida Y. Epidermal sphingolipids: metabolism, function, and roles in skin disorders. FEBS Lett. 2006; 580:5456–5466. [PubMed: 16962101]

Jia Z, Moulson CL, Pei Z, et al. Fatty acid transport protein 4 is the principal very long chain fatty acyl-CoA synthetase in skin fibroblasts. J Biol Chem. 2007; 282:20573–20583. [PubMed: 17522045]

Kazantzis M, Stahl A. Fatty acid transport proteins, implications in physiology and disease. Biochim Biophys Acta. 2012; 1821:852–857. [PubMed: 21979150]

Khnykin D, Ronnevig J, Johnsson M, et al. Ichthyosis prematurity syndrome: clinical evaluation of 17 families with a rare disorder of lipid metabolism. J Am Acad Dermatol. 2012; 66:606–616. [PubMed: 21856041]

Kim JK, Gimeno RE, Higashimori T, et al. Inactivation of fatty acid transport protein 1 prevents fat-induced insulin resistance in skeletal muscle. J Clin Invest. 2004; 113:756–763. [PubMed: 14991074]

Klar J, Schweiger M, Zimmerman R, et al. Mutations in the fatty acid transport protein 4 gene cause the ichthyosis prematurity syndrome. Am J Hum Genet. 2009; 85:248–253. [PubMed: 19631310]

Lin MH, Chang KW, Lin SC, et al. Epidermal hyperproliferation in mice lacking fatty acid transport protein 4 (FATP4) involves ectopic EGF receptor and STAT3 signaling. Dev Biol. 2010; 344:707–719. [PubMed: 20513444]

Lin MH, Hsu FF, Miner JH. Requirement of fatty acid transport protein 4 for development, maturation, and function of sebaceous glands in a mouse model of ichthyosis prematurity syndrome. J Biol Chem. 2013; 288:3964–3976. [PubMed: 23271751]

Lin MH, Khnykin D. Fatty acid transporters in skin development, function and disease. Biochim Biophys Acta. 2013

Macala LJ, Yu RK, Ando S. Analysis of brain lipids by high performance thin-layer chromatography and densitometry. J Lipid Res. 1983; 24:1243–1250. [PubMed: 6631248]

Mihalik SJ, Steinberg SJ, Pei Z, et al. Participation of two members of the very long-chain acyl-CoA synthetase family in bile acid synthesis and recycling. J Biol Chem. 2002; 277:24771–24779. [PubMed: 11980911]

Milger K, Herrmann T, Becker C, et al. Cellular uptake of fatty acids driven by the ER-localized acyl-CoA synthetase FATP4. J Cell Sci. 2006; 119:4678–4688. [PubMed: 17062637]

Moulson CL, Lin MH, White JM, et al. Keratinocyte-specific expression of fatty acid transport protein 4 rescues the wrinkle-free phenotype in Slc27a4/Fatp4 mutant mice. J Biol Chem. 2007; 282:15912–15920. [PubMed: 17401141]

Moulson CL, Martin DR, Lugus JJ, et al. Cloning of wrinkle-free, a previously uncharacterized mouse mutation, reveals crucial roles for fatty acid transport protein 4 in skin and hair development. Proc Natl Acad Sci U S A. 2003; 100:5274–5279. [PubMed: 12697906]

Newberry EP, Xie Y, Kennedy S, et al. Decreased hepatic triglyceride accumulation and altered fatty acid uptake in mice with deletion of the liver fatty acid-binding protein gene. J Biol Chem. 2003; 278:51664–51672. [PubMed: 14534295]

Schmuth M, Ortegon AM, Mao-Qiang M, et al. Differential expression of fatty acid transport proteins in epidermis and skin appendages. J Invest Dermatol. 2005; 125:1174–1181. [PubMed: 16354187]

Sobol M, Dahl N, Klar J. FATP4 missense and nonsense mutations cause similar features in Ichthyosis Prematurity Syndrome. BMC Res Notes. 2011; 4:90. [PubMed: 21450060]

Tao J, Koster MI, Harrison W, et al. A spontaneous Fatp4/Scl27a4 splice site mutation in a new murine model for congenital ichthyosis. PLoS ONE. 2012; 7:e50634. [PubMed: 23226340]

Zhan T, Poppelreuther M, Ehehalt R, et al. Overexpressed FATP1, ACSVL4/FATP4 and ACSL1 increase the cellular fatty acid uptake of 3T3-L1 adipocytes but are localized on intracellular membranes. PLoS ONE. 2012; 7:e45087. [PubMed: 23024797]

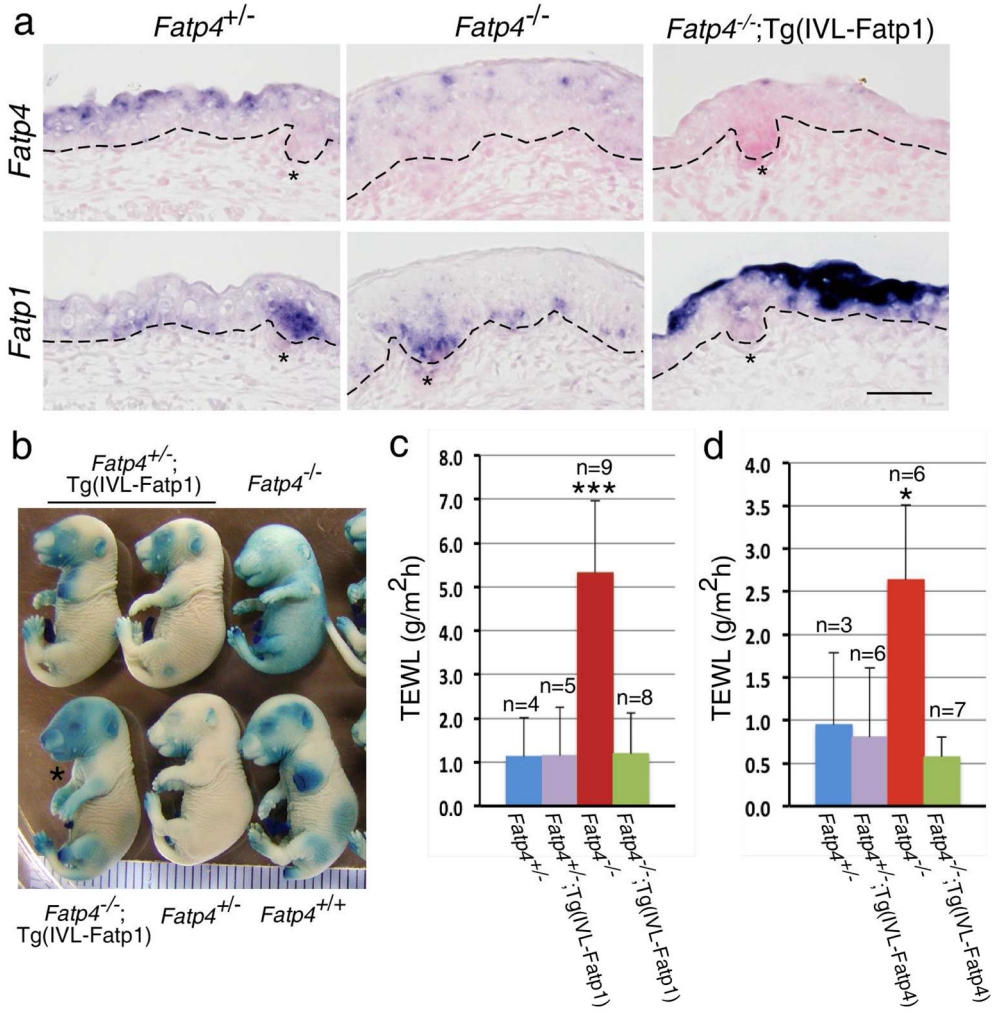

Figure 1. Restoration of the skin barrier in *Fatp4*$^{-/-}$;Tg(IVL-Fatp1) and *Fatp4*$^{-/-}$;Tg(IVL-Fatp4) mice

(a) Dorsal skin sections from E16.0 littermate embryos were subjected to in situ hybridization and counterstained with nuclear fast red. Fatp4 RNA was detected in suprabasal keratinocytes of *Fatp4*$^{+/-}$ (control) and in nuclei of some *Fatp4*$^{-/-}$ keratinocytes (top panels). Fatp1 RNA was detected in basal keratinocytes and hair follicle (asterisks) progenitors of *Fatp4*$^{+/-}$ and *Fatp4*$^{-/-}$ embryos, and additionally detected in suprabasal keratinocytes of *Fatp4*$^{-/-}$;Tg(IVL-Fatp1) embryos (lower panels). Dashed lines demarcate the dermo-epidermal boundary. Scale bar is 50 μm. (b) E17.5 littermate embryos were tested for inward X-Gal permeability. The incomplete barrier in *Fatp4*$^{-/-}$ embryos was remedied in *Fatp4*$^{-/-}$;Tg(IVL-Fatp1) embryos (asterisk). (c, d) Newborns were tested for outward TEWL assays. The increased TEWL in *Fatp4*$^{-/-}$ newborns compared to *Fatp4*$^{+/-}$ controls was normalized in both *Fatp4*$^{-/-}$;Tg(IVL-Fatp1) (c) and *Fatp4*$^{-/-}$;Tg(IVL-Fatp4) newborns (d). Numbers of samples (n) are indicated. ***P<0.001; *P<0.05. The TEWL readings in c and d were obtained from two separate Vapometers.

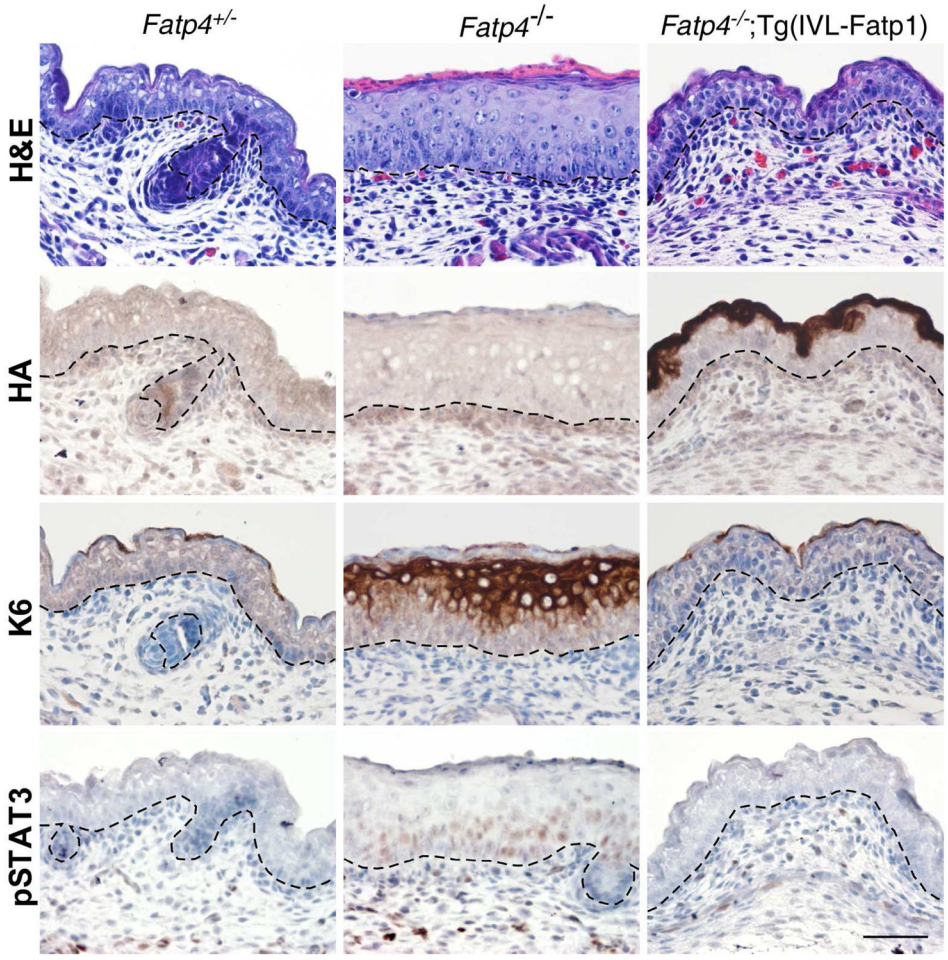

Figure 2. Amelioration of skin phenotypes in *Fatp4*$^{-/-}$;Tg(IVL-Fatp1) mice

Dorsal skin sections from E16.0 embryo littermates were subjected to hematoxylin and eosin staining (top row) and immunohistochemical analyses followed by counterstaining with hematoxylin (bottom three rows). The thickened epidermis phenotype seen in *Fatp4*$^{-/-}$ newborns was normalized in *Fatp4*$^{-/-}$;Tg(IVL-Fatp1) newborns (top row). The HA-tagged FATP1 encoded by the transgene was detected primarily in granular keratinocytes in *Fatp4*$^{-/-}$;Tg(IVL-Fatp1) mice (second row). The ectopic expression of keratin 6 seen in *Fatp4*$^{-/-}$ newborns was diminished in *Fatp4*$^{-/-}$;Tg(IVL-Fatp1) mice (third row). The nuclear localization of pSTAT3 shown in *Fatp4*$^{-/-}$ newborns was also diminished in *Fatp4*$^{-/-}$;Tg(IVL-Fatp1) mice (bottom row). Dashed lines demarcate the dermo-epidermal boundary. Scale bar is 50 μm.

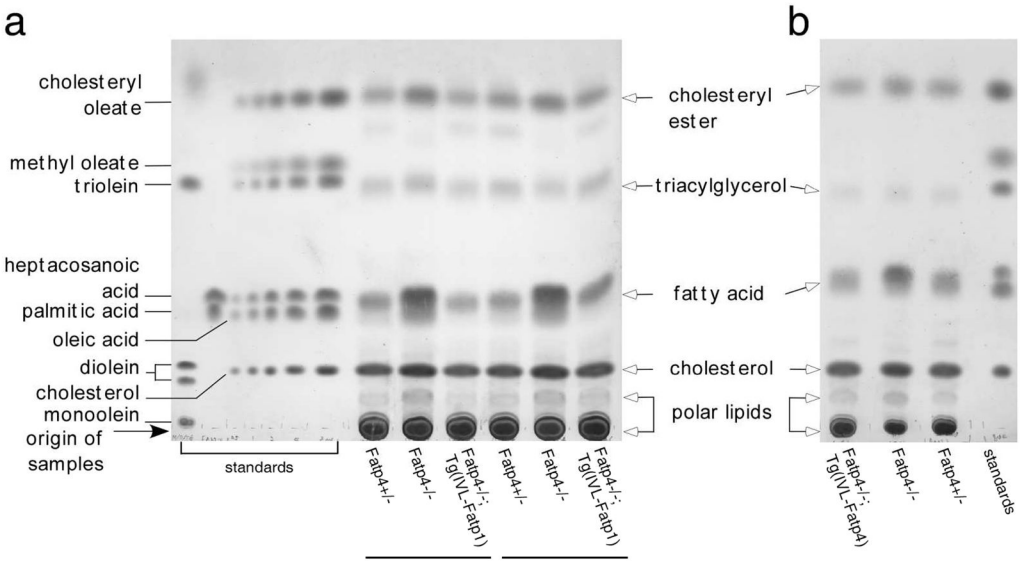

Figure 3. Amelioration of the elevated level of free fatty acids in *Fatp4*$^{-/-}$;Tg(IVL-Fatp1) and *Fatp4*$^{-/-}$;Tg(IVL-Fatp4) epidermis

Free, extractable lipids from the epidermis of newborn mice were resolved by TLC and visualized by charring the plate. The elevated level of free fatty acids seen in *Fatp4*$^{-/-}$ mice was reduced to normal in *Fatp4*$^{-/-}$;Tg(IVL-Fatp1) (a) and *Fatp4*$^{-/-}$;Tg(IVL-Fatp4) mice (b). Components of the lipid standards and origin of sample application are indicated on the left of a. Lipid species of the epidermis are indicated between the panels.

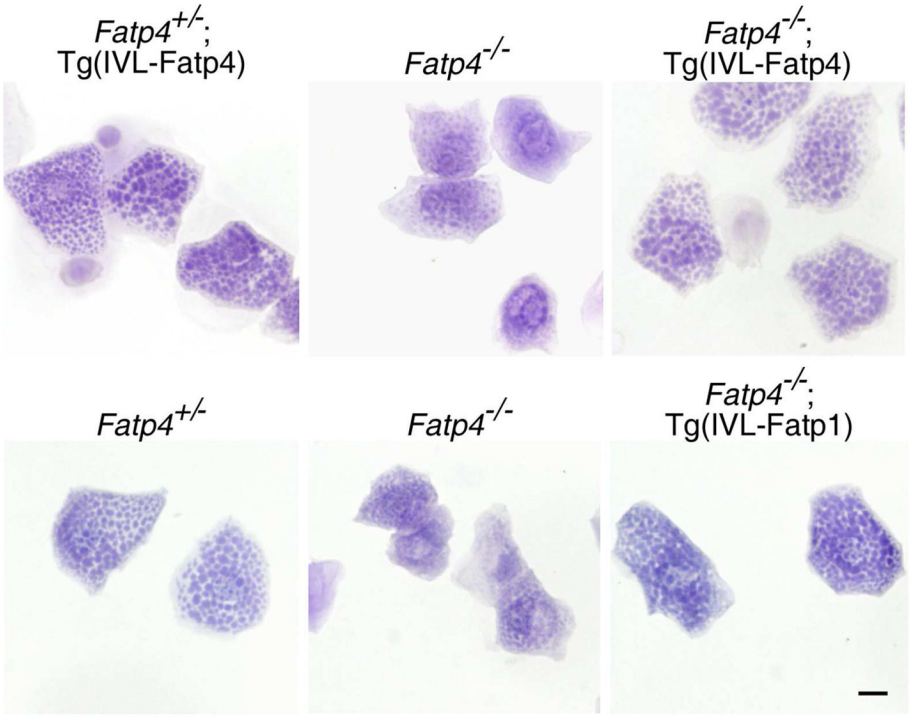

Figure 4. Restoration of the keratohyalin granules in *Fatp4*$^{-/-}$;Tg(IVL-Fatp4) and *Fatp4*$^{-/-}$;Tg(IVL-Fatp1) mice

Granular keratinocytes-enriched cell fractions were prepared from the epidermis of newborn littermates and stained with hematoxylin. The smaller cell size and less distinct keratohyalin granules seen in *Fatp4*$^{-/-}$ mice compared to control (*Fatp4*$^{+/-}$) were normalized in *Fatp4*$^{-/-}$;Tg(IVL-Fatp4) and *Fatp4*$^{-/-}$;Tg(IVL-Fatp1) mice. Scale bar is 10 μm.

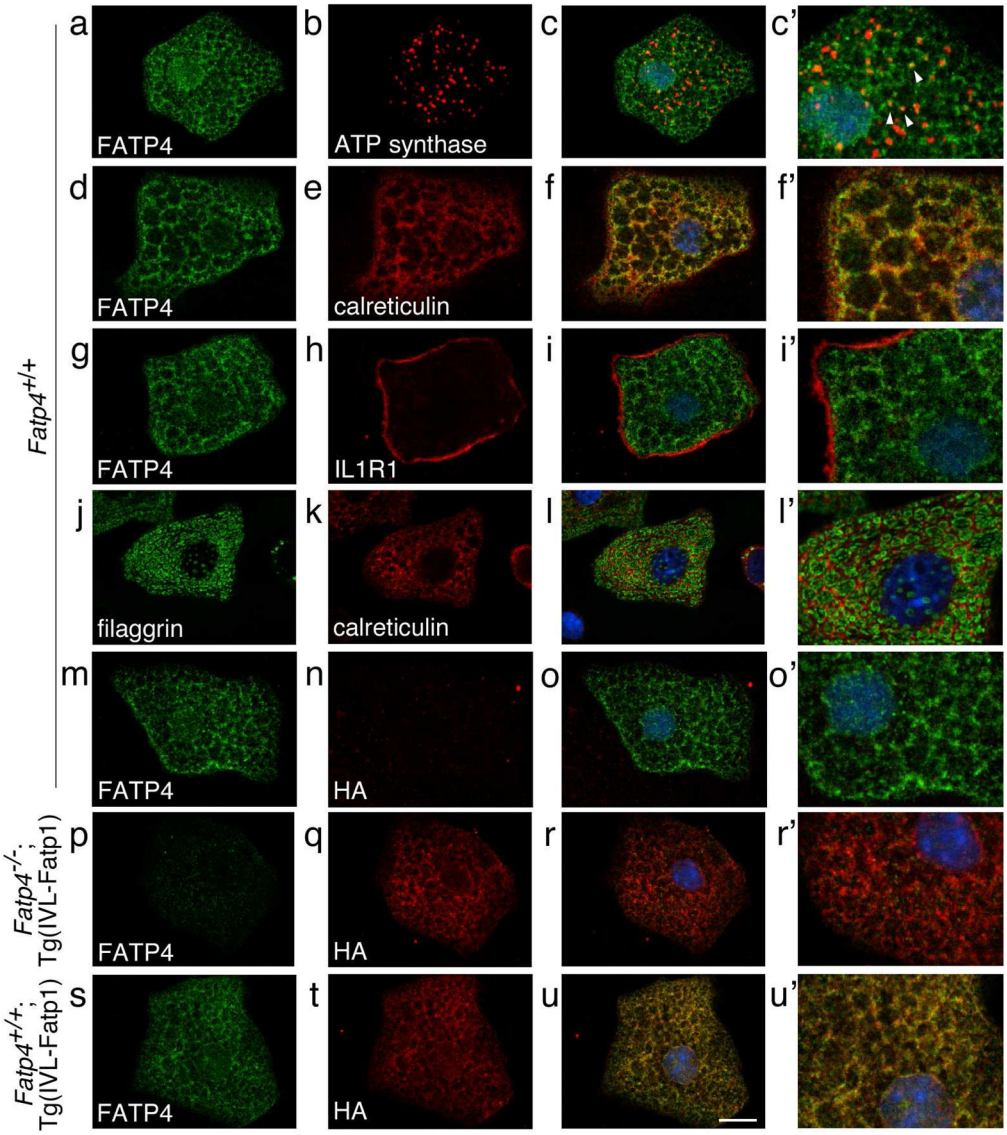

Figure 5. Subcellular localization of endogenous FATP4 and transgenic FATP1 in granular keratinocytes

Granular keratinocytes from the epidermis of newborns (a–i′, m–o′) or 1.5 (j–l′) or 5.5-day-old (p–u′) pups were subjected to double immunofluorescence staining with the indicated antibodies. Merged confocal images of low and high magnification are shown in the right two columns. The mesh-like pattern of FATP4 staining in *Fatp4*$^{+/+}$ cells colocalized partially with the mitochondrial membrane protein ATP synthase (a–c′; arrowheads in c′) and mainly with the ER luminal protein calreticulin (d–f′), but not with the plasma membrane protein interleukin 1 receptor 1 (g–i′). The mesh-like pattern of FATP4 localization was similar to the staining pattern of calreticulin around the filaggrin-positive granules (j–l′). The HA-tagged FATP1 in *Fatp4*$^{+/+}$;Tg(IVL-Fatp1) cells also showed a mesh-like staining pattern that colocalized with endogenous FATP4 (s–u′). The HA-tagged

FATP1 was not detected in *Fatp4*$^{+/+}$ cells (m–o′). Endogenous FATP4 was not detected in *Fatp4*$^{-/-}$;Tg(IVL-Fatp1) cells (p–r′). Scale bar is 10 μm.